



# Enhanced production of 3,4-dihydroxybutyrate from xylose by engineered yeast via xylonate re-assimilation under alkaline condition

Yukawa, Takahiro ; Bamba, Takahiro ; Matsuda, Mami ; Yoshida, Takanobu ; Inokuma, Kentaro ; Kim, Jungyeon ; Won Lee, Jae ; Jin, Yong-Su ;...

---

**(Citation)**

Biotechnology and Bioengineering, 120(2):511-523

**(Issue Date)**

2023-02

**(Resource Type)**

journal article

**(Version)**

Accepted Manuscript

**(Rights)**

This is the peer reviewed version of the following article: [Yukawa, T., Bamba, T., Matsuda, M., Yoshida, T., Inokuma, K., Kim, J., Won Lee, J., Jin, Y.-S., Kondo, A., & Hasunuma, T. (2023). Enhanced production of 3,4-dihydroxybutyrate from xylose by engineered yeast via xylonate re-assimilation under alkaline condition. Biotechnolog...

**(URL)**

<https://hdl.handle.net/20.500.14094/0100478206>



1 **Title:**

2 Enhanced production of 3,4-dihydroxybutyrate from xylose by engineered yeast  
3 via xylonate re-assimilation under alkaline condition

4 **Authors:**

5 Takahiro Yukawa<sup>a</sup>, E-mail: 188p016p@stu.kobe-u.ac.jp

6 Takahiro Bamba<sup>a</sup>, E-mail: t.bamba@bear.kobe-u.ac.jp

7 Mami Matsuda<sup>a,b</sup>, E-mail: matsuda\_mami@harbor.kobe-u.ac.jp

8 Takanobu Yoshida<sup>a</sup>, E-mail: t-yoshida@port.kobe-u.ac.jp

9 Kentaro Inokuma<sup>a</sup>, E-mail: kinokuma@port.kobe-u.ac.jp

10 Jungyeon Kim<sup>c, d</sup> E-mail: jungyeon@illinois.edu

11 Jae Won Lee<sup>c, d</sup> E-mail: jlee762@illinois.edu

12 Yong-Su Jin<sup>c, d</sup> E-mail: ysjin@illinois.edu

13 Akihiko Kondo<sup>a, b, e</sup> E-mail: akondo@kobe-u.ac.jp

14 Tomohisa Hasunuma<sup>a, b, e</sup>, E-mail: hasunuma@port.kobe-u.ac.jp

15 **Affiliations**

16 <sup>a</sup> Graduate School of Science, Technology and Innovation, Kobe University, 1-1  
17 Rokkodai, Nada, Kobe 657-8501, Japan

18 <sup>b</sup> Engineering Biology Research Center, Kobe University, 1-1 Rokkodai, Nada,  
19 Kobe, 657-8501, Japan

20 <sup>c</sup> Department of Food Science and Human Nutrition, University of Illinois at  
21 Urbana-Champaign, Urbana, IL, USA.

22 <sup>d</sup> Carl R. Woese Institute for Genomic Biology, University of Illinois at Urbana-  
23 Champaign, Urbana, IL, USA.

24 <sup>e</sup> RIKEN Center for Sustainable Resource Science, 1-7-22 Suehiro-cho, Tsurumi-  
25 ku, Yokohama, Kanagawa 230-0045, Japan

26 **Corresponding author**

27 Tomohisa Hasunuma

28 Engineering Biology Research Center, Kobe University

29 1-1 Rokkodai, Nada, Kobe 657-8501, Japan

30 hasunuma@port.kobe-u.ac.jp

### 31 **Funding**

32 This work was funded by project P16009 (Development of production techniques  
33 for highly functional biomaterials using plant and other organism smart cells) and  
34 P20011 (Development of bio-derived product production technology that  
35 accelerates the realization of carbon recycling) from the New Energy and  
36 Industrial Technology Development Organization (NEDO). TH was also  
37 supported by Grant-in-Aid for Scientific Research (B) (JP21H01729) from the  
38 Japan Society for the Promotion of Science (JSPS). TY was supported by JSPS  
39 Grant-in-Aid for JSPS Fellows (JP21J10891).

### 40 **Abstract**

41 To realize lignocellulose-based bioeconomy, efficient conversion of xylose into  
42 valuable chemicals by microbes is necessary. Xylose oxidative pathways that  
43 oxidize xylose into xylonate can be more advantageous than conventional xylose  
44 assimilation pathways because of fewer reaction steps without loss of carbon and  
45 ATP. Moreover, commodity chemicals like 3,4-dihydroxybutyrate and 3-  
46 hydroxybutyrolactone can be produced from the intermediates of xylose oxidative  
47 pathway. However, successful implementations of xylose oxidative pathway in  
48 yeast have been hindered because of the secretion and accumulation of xylonate  
49 which is a key intermediate of the pathway, leading to low yield of target product.  
50 Here, high-yield production of 3,4-dihydroxybutyrate from xylose by engineered  
51 yeast was achieved through genetic and environmental perturbations.  
52 Specifically, 3,4-dihydroxybutyrate biosynthetic pathway was established in yeast  
53 through deletion of *ADH6* and overexpression of *yne1*. Also, inspired by the  
54 mismatch of pH between host strain and key enzyme of XylID, alkaline

55 fermentations ( $\text{pH} \geq 7.0$ ) were performed to minimize xylonate accumulation.  
56 Under the alkaline conditions, xylonate was re-assimilated by engineered yeast  
57 and combined product yields of 3,4-dihydroxybutyrate and 3-  
58 hydroxybutyrolactone resulted in 0.791 mol/mol-xylose, which is highest  
59 compared with previous study. These results shed light on the utility of the xylose  
60 oxidative pathway in yeast.

61

62 **KEYWORDS**

63 3,4-Dihydroxybutyrate, 3-Hydroxybutyrolactone, Xylonate assimilation, Xylose  
64 oxidative pathway, *Saccharomyces cerevisiae*

65

## 66 1 | INTRODUCTION

67 For the sustainable production of commodity chemicals, replacing petrochemical-  
68 based industry with renewable biomass-based bioconversion is becoming an  
69 important proposition. Traditionally, starch and sugarcane have been used as  
70 feedstocks for microbial fermentation to produce biochemicals. However, using  
71 human-edible portions of crops may result in social and ethical issues such as  
72 unstable supply and fluctuating prices of foods. Therefore, non-edible biomass  
73 has received increasing attention as sustainable feedstocks for developing next-  
74 generation biorefineries (Protzko et al., 2018; Sun et al., 2021; Wei et al., 2013).  
75 Especially, lignocellulosic biomass, mainly composed of 30-50 % glucose, 20-  
76 25 % xylose, is one of the most abundant feedstocks on earth (Lane et al., 2018).

77         Glucose and xylose can be converted into various of bio-derived  
78 compounds via a conventional xylose pathway (Lee et al., 2022). However,  
79 xylose fermentation by an engineered yeast strain was much inferior to glucose  
80 fermentation because of many limiting factors such as carbon catabolite  
81 repression by glucose, redox imbalances, and by-product formation (Kim et al.,  
82 2013). In addition, conventional xylose assimilation pathway, utilizing xylose  
83 isomerase and xylose reductase/xylitol dehydrogenase, require the use of ATP  
84 when the metabolite enter central metabolic pathways such as pentose  
85 phosphate pathway (PPP) and glycolysis (Shen et al., 2020).

86         Recently, a xylose oxidative pathway has been identified as a novel non-  
87 phosphorylative pathway in recombinant microbial strains (Watanabe et al.,  
88 2019) (Fig. 1). The xylose oxidative pathway does not require ATP for shunting  
89 xylose into central metabolism, and the pathway is independent of the inherent  
90 glycolysis and PPP (Shen et al., 2020). As shown in Fig. 1, xylose is oxidized into  
91 2-keto-3-deoxy-xylonate (KDX) and further converted to either  $\alpha$ -ketoglutarate via  
92 the Weimberg pathway (Weimberg, 1961), or pyruvate and glycolaldehyde via

93 the Dahms pathway (Dahms, 1974). The xylose oxidative pathway has a potential  
94 to produce chemicals such as 3,4-dihydroxybutyrate (3,4-DHBA) (Wang et al.,  
95 2017), 1,2,4-butanetriol (BT) (Yukawa et al., 2021), ethylene glycol, or glycolate  
96 (Salusjärvi et al., 2017) from xylose (Fig. 1).

97 3,4-DHBA and its lactonized form 3-hydroxybutyrolactone (3-HBL) are  
98 versatile chemicals as 3-HBL is listed as one of the top value-added biochemicals  
99 in the report by U. S. Department of Energy (Werpy and Petersen, 2004). 3-HBL  
100 can be polymerized to produce polyhydroxyalkanoates, and it can be used as  
101 precursors for synthesizing chiral drugs (Dhamankar et al., 2014). The microbial  
102 production of 3-HBL and 3,4-DHBA from glucose and glycolate in *E. coli* was  
103 firstly reported in 2013 (Martin et al., 2013), and subsequently achieved 0.32 g/L  
104 of 3-HBL and 0.70 g/L of 3,4-DHBA from solely 10 g/L glucose (Dhamankar et  
105 al., 2014). However, multiple reaction steps and low substrate specificity of  
106 enzymes resulted in low yields and the formation of many by-products  
107 (Dhamankar et al., 2014). In contrast, 3,4-DHBA production from xylose is more  
108 desirable because of the 100 % theoretical yield from xylose and its  
109 independence from glucose metabolism (Shen et al., 2020). Previously, 3,4-  
110 DHBA synthetic pathway from xylose was established in *E. coli* (Wang et al.,  
111 2017), and the integration of a fusion enzyme consisting of KDX decarboxylase  
112 (PpMdlC) and xylonate dehydratase (YagF) resulted in a titer of 7.71 g/L of 3,4-  
113 DHBA from 20 g/L of xylose with a molar yield of 60 % (Liu et al., 2021) (Table  
114 2).

115 The xylose oxidative pathway has been introduced into bacterial strains  
116 such as *Escherichia coli* (Fujiwara et al., 2020) and *Corynebacterium glutamicum*  
117 (Brüsseler et al., 2019). Also, resulting strain in previous study exhibit good  
118 growth from xylose as a sole carbon source (Tai et al., 2016) and product titers  
119 and yields (Bai et al., 2016; Choi et al., 2016) with xylonate re-assimilation

120 (Bañares et al., 2021). The yeast *S. cerevisiae* is also desirable host strain for  
121 producing cellulosic biochemicals due to its high tolerance to fermentation  
122 inhibitors and no bacteriophage infection (Hong and Nielsen, 2012; Sharma et al.,  
123 2022). Indeed, engineered yeast could be more suitable for the production of bio-  
124 based chemicals from pretreated and hydrolyzed biomass as compared to  
125 engineered *E. coli* (Bamba et al. 2019). On the other hand, the engineered yeast  
126 strains accumulated excessive amounts of xylonate in the medium without  
127 xylonate re-assimilation (Bamba et al., 2019, Salusjärvi et al., 2017). Xylonate  
128 converted from xylose was immediately released outside the yeast cells before  
129 conversion to KDX. As such, productions of target molecules by engineered *S.*  
130 *cerevisiae* strains were not impressive (Salusjärvi et al., 2017; Yukawa et al.,  
131 2021, Table 2). Notably, the engineered yeast strains could not grow on xylose  
132 as a carbon source via Weimberg pathway (Borgström et al., 2019). These  
133 studies indicate that more improvement is necessary to realize more efficient  
134 xylose conversion with less xylonate accumulation via oxidative xylose pathway  
135 in *S. cerevisiae*.

136 To relieve xylonate accumulation by engineered *S. cerevisiae* strain, the  
137 enhancement in the activity of *Caulobacter crescentus* XylID has been needed.  
138 For example, strain engineering is effective by deleting *BOL2*, encoding  
139 transcriptional repressor of iron regulon, to enhance cellular iron uptake into the  
140 yeast cells (Kumánovics et al., 2008). In addition to the deletion of *BOL2*, the  
141 overexpression of a truncated *TYW1* (*tTYW1*), which enhances iron uptake in  
142 yeast (Li et al., 2011), more improved *C. crescentus* XylID activity (Bamba et al.,  
143 2019). Although the combination of *BOL2* deletion with *tTYW1* overexpression  
144 further improved XylID activity *in vitro*, this genetic perturbation did not lead to a  
145 higher titer of BT (Bamba et al., 2019). Although an *in vitro* enzyme assay is a  
146 powerful tool to confirm the expression of an active enzymes, the improvement

147 of *in vitro* enzyme activity does not always guarantee increased expression of the  
148 pathway *in vivo* or product titers. This might be due to the differences in the  
149 reaction environments between *in vitro* and *in vivo*. Notably, although the optimal  
150 pH range of *C. crescentus* XylD activity is reported to be from pH 7.0 to 9.0 by *in*  
151 *vitro* assay (Andberg et al., 2016), *S. cerevisiae* strains harboring a xylose  
152 oxidative pathway were conventionally cultivated in a pH range lower than 6.0  
153 because of the acidification of the fermentation medium by the multiple factors,  
154 for example, the use of ammonium ion as a nitrogen source (Hensing et al., 1995).  
155 In addition, the effects of pH on xylose oxidative pathway in yeast have not been  
156 reported yet.

157         Here, we demonstrated the cultivation of engineered *S. cerevisiae* with a  
158 xylose oxidative pathway under weak alkaline conditions can induce extracellular  
159 xylonate import to the cells, leading to the increase of the intracellular availability  
160 of KDX and 3,4-DHBA production from xylose. As a result, 3,4-DHBA and 3-HBL  
161 titer reached at 6.5 and 0.20 g/L from 10.9 g/L xylose with a total molar yield of  
162 79.1 % without xylonate accumulation after 120 h fermentation. These results  
163 demonstrate an effective strategy to reduce the accumulation of intermediates for  
164 accelerating the biorefinery via the xylose oxidative pathway in yeast and provide  
165 a new insight into how heterologous pathway fluxes can be altered in a host strain  
166 through environmental perturbations.

## 167 **2 | MATERIALS AND METHODS**

### 168 **2.1 | Chemicals**

169 Due to the commercial unavailability of (*R*)-3,4-DHBA, the 3,4-DHBA standard  
170 was prepared as described in the previous study (Martin et al., 2013). 3-HBL  
171 purchased from Alfa Aesar (Ward Hill, Massachusetts, USA). Xylonate and KDX  
172 were purchased from Toronto Research Chemicals (North York, Canada) and  
173 Sigma-Aldrich (St. Louis, MO, USA), respectively. In addition, unless otherwise



174 stated, all chemicals were purchased from Nacalai Tesque (Kyoto, Japan). 3,4-  
175 Dihydroxybutanal (DHB) was identified by a capillary electrophoresis time-of-  
176 flight mass spectrometry (CE-TOFMS) at  $m/z = 103.0391$  due to the unavailability  
177 of an authentic DHB standard.

## 178 **2.2 | Strains and plasmid constructions**

179 *E. coli* NovaBlue (Merck Millipore, Darmstadt, Germany) was used for plasmid  
180 construction. All plasmids were constructed by using the In-fusion HD cloning kit  
181 (Takara Bio USA, Mountain View, CA, USA), according to the recommended  
182 protocol. Codon-optimized *C. crescentus xyIB* and *xyID*, and *Lactococcus lactis*  
183 *kdcA* for *S. cerevisiae* have been previously obtained (Bamba et al., 2019).  
184 Codon-optimized *E. coli yneI* and *sf* for *S. cerevisiae* was synthesized by Geneart  
185 (Thermo Fisher Scientific, Waltham, MA, USA).

186 *S. cerevisiae* YPH499 (Stratagene, La Jolla, CA, USA) was used in this  
187 study. All yeast strains used in this study and their descriptions are summarized  
188 in Table 1. The details of plasmid and strain construction were specified in  
189 Supplemental Text S1 and Text S2.

## 190 **2.3 | Shake-flask fermentation**

191 Shake flask fermentation was conducted in a 200-mL baffled Erlenmeyer flask as  
192 described in the previous study (Bamba et al., 2019). Briefly, fermentation was  
193 performed in 20 mL of the YPDX medium containing 10 g/L yeast extract, 20 g/L  
194 Bactopectone (Difco Laboratories), 10 g/L glucose and 10 g/L xylose with an initial  
195  $OD_{600} = 5.0$ . The 1.0 mL culture was collected at every sampling point to  
196 determine the amounts of metabolites.

## 197 **2.4 | Batch fermentation in bioreactor**

198 Batch fermentation was performed using Bio Jar.8 (ABLE Biott, Tokyo, Japan)  
199 with an initial working volume of 100 mL. Yeast cells grown in 400 mL YPD  
200 medium at 30 °C were collected by centrifugation at 2,200×g for 5 min and

201 washed by 10 mL distilled water twice. The washed cells were inoculated into the  
202 medium with initial  $OD_{600} = 5.0$ . The medium was composed of 10 g/L yeast  
203 extract, 20 g/L Bactopeptone, 10 g/L glucose and 10 g/L xylose at 0 h. Antifoam  
204 SI (FUJIFILM Wako Pure Chemical, Ltd., Osaka, Japan) was appropriately added.  
205 The temperature was controlled at 30 °C. The pH of culture was maintained by  
206 the automatic addition of a 5 N NaOH or 5N KOH. The airflow was maintained at  
207 100 mL/min with compressed air. The culture medium was sampled every 24 h,  
208 to determine metabolite concentrations and cell density ( $OD_{600}$ ) using a  
209 spectrophotometer.

## 210 **2.5 | Metabolite analysis**

211 The amounts of xylonate, BT, 3,4-DHBA and 3-HBL in the medium were analyzed  
212 by GC-MS (GCMS-QP 2010 Ultra; Shimadzu, Kyoto, Japan), and the running  
213 condition was described in the previous previously (Bamba et al., 2019).

214 Glucose and xylose concentrations in the medium were measured using  
215 high-performance liquid chromatography (HPLC) (Shimadzu, Kyoto, Japan) with  
216 a RID-10A refractive index detector (Shimadzu) equipped with an Eclipse XDB-  
217 C18 column (4.6 mm × 250 mm, particle size 5 μm; Agilent Technologies,  
218 Hercules, CA, USA). The HPLC system was operated at 80 °C, with a ultrapure  
219 water as the mobile phase at a flow rate of 0.6 mL/min.

220 CE-TOFMS (CE, Agilent G7100; MS, Agilent G6224AA LC/MSD TOF;  
221 Agilent Technologies, Palo Alto, CA, USA) was used to measure the amounts of  
222 intracellular xylonate, KDX,  $NAD^+$ ,  $NADP^+$  and extracellular KDX analysis. The  
223 method to extract metabolites from the medium (Yukawa et al., 2021) and cells  
224 (Inokuma et al., 2018), and running parameters (Hasunuma et al., 2013) was  
225 described in the previous reports.

226 pH in the fermentation medium was determined using compact pH meter  
227 (LAQUA twin, HORIBA, Kyoto, Japan). The method of intracellular pH analysis

228 was described previously (Reifenrath & Boles, 2018), specified in Supplemental  
229 Materials (Text S4).

### 230 **3 | RESULTS AND DISCUSSION**

#### 231 **3.1 | A pathway design to produce 3,4-dihydroxybutyrate from xylose in** 232 **engineered yeast.**

233 The 3,4-DHBA biosynthetic pathway from xylose is based on xylose oxidative  
234 pathway (Fig. 1). Xylose is converted into xylonolactone by xylose  
235 dehydrogenase XylB and xylonolactone is further converted into xylonate by the  
236 spontaneous reaction. Xylonate is then converted into KDX by xylonate  
237 dehydratase XylD, and KDX is catalyzed into 3,4-dihydroxybutanal (DHB) by 2-  
238 ketoacid decarboxylase. Previously, *Lactococcus lactis* KdcA is suitable for the  
239 decarboxylation of KDX to DHB (Bamba et al., 2019). Finally, DHB is converted  
240 into the 3,4-DHBA by aldehyde dehydrogenase (ALD). We first constructed the  
241 BDK strain harboring one copy of *C. crescentus* XylB, XylD, and *L. lactis* KdcA  
242 for the assessment of further study.

#### 243 **3.2 | Blocking the formation of by-product 1,2,4-butanetriol in engineered** 244 **yeast through the knockout of alcohol dehydrogenase**

245 To construct an efficient 3,4-DHBA biosynthetic pathway with high yield from  
246 xylose, the conversion of medium-chain aldehyde of DHB into a medium-chain  
247 alcohol BT by endogenous enzymes in yeast needs to be eliminated (Wang et  
248 al., 2017). Interruption of the reaction from DHB to yield BT would be critical  
249 because substantial amounts of BT were produced in the medium as a by-  
250 product by engineered *E. coli* (Wang et al., 2017). However, the enzymes  
251 responsible for catalyzing this reaction in *S. cerevisiae* have not been identified  
252 yet. In *S. cerevisiae*, Adh(s) catalyze the reversible reactions of aldehydes to  
253 alcohols such as well-characterized Adh1 to Adh7 (de Smidt et al., 2008). For  
254 example, Adh6 and Adh7 are known to exhibit broad substrate specificities

255 (Larroy et al., 2002a; Larroy et al., 2002b). Although substrate specificities of  
256 Adh(s) in *S. cerevisiae* have been investigated, no ADH(s) is known to recognize  
257 unnatural compounds such as DHB (Niu et al., 2003).

258 In order to reduce the formation of BT, we screened Adh(s) enzymes that  
259 might catalyze BT formation by disrupting each *ADH* genes in the BDK strain. To  
260 construct a *ADH* deletion library, each *ADH* gene from *ADH1* to *ADH7* was  
261 disrupted in the BDK strain, respectively. We performed glucose and xylose co-  
262 fermentation and examined the xylose consumption and BT production by the  
263 ADH disrupted strain (Fig. 2A and 2B). The parental BDK strain produced 0.22  
264 g/L of BT from 10.6 g/L xylose at 96 h (Fig. 2A and 2B). Deletion of *ADH2*, *ADH5*,  
265 or *ADH7* did not change the titers of BT. Interestingly, the deletion of *ADH3* had  
266 a positive effect on BT production, and the BT titer reached 0.29 g/L after 96 h  
267 fermentation (Fig. 2B). In contrast, the deletion of *ADH1*, *ADH4*, and *ADH6*  
268 reduced the titers of BT after 96 h fermentation as compared with the parental  
269 BDK strain. In particular, the BDK $\Delta$ 6 with the deletion of *ADH6* produced BT only  
270 at 0.01 g/L (Fig. 2B). Deletion of *ADH1* also reduced the xylose consumption (Fig.  
271 2A), leading to the low BT production (Fig. 2B). Deletion of *ADH4* also reduced  
272 BT titer at 0.18 g/L (Fig. 2B). In particular, the titer of BT was dropped from 0.22  
273 g/L of BDK strain to 0.01 g/L of BDK $\Delta$ 6 strain at 96 h by the deletion of *ADH6*  
274 (Fig. 2B). These results suggest that *ADH6* is a deletion target for a high yield  
275 production of 3,4-DHBA by engineered yeast. However, the BDK $\Delta$ 6 strain did not  
276 produce 3,4-DHBA. This suggested further engineering is required for 3,4-DHBA  
277 production.

### 278 **3.3 | Increased fluxes from xylonate to 3,4-dihydroxybutanal enable the** 279 **production of 3,4-dihydroxybutyrate in engineered yeast**

280 Previously, we developed the BD $\delta$ K603 strain for the production of BT (Yukawa  
281 et al., 2021). This strain harbors one copy of *C. crescentus* XylB and XylD, and

282 six copies of *L. lactis* KdcA. In addition, iron metabolism was modified with the  
283 deletion of *BOL2* and the overexpression of *tTYW1* to improve the activity of iron-  
284 sulfur protein XylD (Bamba et al., 2019; Yukawa et al., 2021). As the BDδK603  
285 strain exhibits higher fluxes from xylose to DHB (Yukawa et al., 2021), we  
286 reasoned that the deletion of *ADH6* in the BDδK603 strain might enable the  
287 production of 3,4-DHBA from xylose.

288 To minimize BT formation while keeping the flux of xylose to DHB in the  
289 BDδK603 strain, *ADH6* gene was deleted in the genome of the BDδK603 strain,  
290 resulting in the construction of the BDδK604 strain. We examined the product  
291 profiles from glucose and xylose fermentation by the parental BDδK603 strain  
292 and *ADH6*-deleted BDδK604 strains. The BDδK603 strain produced 7.4 g/L of  
293 xylonate (Fig. S1) and 1.5 g/L of BT (Fig. 2C). Interestingly, the BDδK603 strain  
294 produced 0.3 g/L of 3,4-DHBA without the deletion of any *ADH*(s) or integration  
295 of ALD catalyzing the reaction from DHB to 3,4-DHBA (Fig. 2D). By the disruption  
296 of *ADH6*, the BDδK604 strain produced 8.2 g/L of xylonate (Fig. S1), 0.3 g/L of  
297 BT (Fig. 2C), and 0.4 g/L of 3,4-DHBA (Fig. 2D). While the deletion of *ADH6*  
298 reduced BT formation from 1.5 to 0.3 g/L of BT (Fig. 2C), the improvement of 3,4-  
299 DHBA production was marginal (Fig. 2D, 0.3 vs. 0.4 g/L of 3,4-DHBA) between  
300 the BDδK603 and BDδK604 strains. The molar yield of 3,4-DHBA in BDδK604  
301 strain was only 0.02 %. While endogenous aldehyde dehydrogenase in yeast  
302 might be converting DHB to 3,4-DHBA (Fig. 2D), heterologous enzyme needs to  
303 be introduced into the BDδK604 strain for the enhanced production of 3,4-DHBA.

### 304 **3.4 | Improvement of 3,4-dihydroxybutyrate production by integration of** 305 **suitable aldehyde dehydrogenase**

306 As the structure of DHB is similar to that of succinate semialdehyde, succinate  
307 semialdehyde dehydrogenase Ynel from *E. coli* was overexpressed to the  
308 increased production of the 3,4-DHBA by engineered *E. coli* (Wang et al., 2017).

309 Thus, the *ynel* was selected as a target gene for the enhanced production of 3,4-  
310 DHBA in *S. cerevisiae*. In addition, we reasoned that endogenous enzymes in *S*  
311 *cerevisiae* such as succinate semialdehyde dehydrogenase of Uga2, NAD<sup>+</sup>-  
312 dependent cytoplasmic ALDs of Ald2 and Ald3 might be responsible for the small  
313 amounts of 3,4-DHBA produced by the BDδK603 and BDδK604 strains (Fig. 2D).  
314 Therefore, Uga2, Ald2, and Ald3 were additionally selected as candidate  
315 enzymes for 3,4-DHBA production.

316 Each gene of *ynel*, *UGA2*, *ALD2* and *ALD3* under the control of *TDH3*  
317 promoter was integrated into the BDδK604 strain, resulting in the construction of  
318 the BDδK604-Ynel, BDδK604-Uga2, BDδK604-Ald2 and BDδK604-Ald3 strains,  
319 respectively. As shown in Fig. 3A, the overexpression of *ynel* enhanced 3,4-  
320 DHBA production at 1.0 g/L from 10.6 g/L of consumed xylose (Fig. S2) with a  
321 molar yield of 11.8 %, which was 2.5-fold higher than the parental strain BDδK604  
322 at 0.4 g/L (Fig. 2D). The overexpression of *UGA2* did not improve the 3,4-DHBA  
323 titer. The overexpression of *ALD2* and *ALD3* also enhanced the carbon flux  
324 toward 3,4-DHBA, producing 0.7 and 0.5 g/L of 3,4-DHBA by the BDδK604-Ald2  
325 and BDδK604-Ald3 strains, respectively. These results suggested that Ynel is  
326 the most effective ALD among the overexpressed enzymes.

327 Xylonate accumulation by these strains changed marginally, but the  
328 overexpression of *ynel* relieved xylonate accumulation at 8.2 g/L (Fig. 3B). This  
329 means that 66.5% of the consumed xylose was wasted into the medium as  
330 xylonate, resulting in the low yield of 3,4-DHBA from xylose by the BDδK604-  
331 Ynel strain. BT formation by the BDδK604-Ynel strain was slightly lower as  
332 compared with those by the other strains, and intracellular pH values and the pool  
333 size of intracellular NAD<sup>+</sup> and NADP<sup>+</sup> at 24 h did not exhibit significant differences  
334 (Fig. S3). Thus, Ynel might have a better substrate specificity for DHB between  
335 the four enzymes. In addition to the change of metabolites, pH of the culture

336 medium of the BD $\delta$ K604-Ynel strain drastically dropped from pH = 6.3 at 0 h to  
337 pH = 4.0 at 96 h (Fig. 3C) because a major by-product xylonate is a weak acid  
338 and is known to acidify fermentation media (Toivari et al., 2012), and final product  
339 3,4-DHBA is also weak acid with a pKa value of 4.09.

### 340 **3.5 | The 3,4-dihydroxybutyrate production under the pH control**

341 Control of oxygen supply and pH of culture media in a lab-scale shake-flask  
342 fermentation is difficult so that our fermentation results for the production of 3,4-  
343 DHBA might not reflect the full potential of the engineered BD $\delta$ K604-Ynel strains.  
344 As such, pH-controlled fermentation in a bioreactor were performed to examine  
345 the production capacity of 3,4-DHBA production by the BD $\delta$ K604-Ynel under  
346 different aeration conditions.

347 Using a bioreactor, fermentation was performed while keeping the lower  
348 limit of pH of the medium was kept at 6.0 by NaOH. The effects of aeration on  
349 the production of 3,4-DHBA by the BD $\delta$ K604-Ynel were evaluated through  
350 changing agitation speeds from 200 to 500 rpm. Dissolved oxygen levels were  
351 controlled corresponding to the agitation speeds (Fig. S4). Glucose was  
352 completely consumed within 24 h by each agitation speed (Fig. S5), and xylose  
353 was sequentially consumed in the fermentation at 500 rpm (Fig. 4A). 5.8 g/L of  
354 xylonate was accumulated (Fig. 4B) and 3.5 g/L of 3,4-DHBA was produced (Fig.  
355 4C). Compared to the result at 500 rpm, fermentations at lower agitation speeds  
356 exhibited the reduced xylose consumption rates, less amounts of accumulated  
357 xylonate, and higher titers of 3,4-DHBA. Notably, the fermentation at 300 rpm  
358 produced 4.6 g/L of 3,4-DHBA with a molar yield of 51.3 % from 11.2 g/L of xylose.  
359 Increase in the production of 3,4-DHBA under low aeration conditions at 300 rpm  
360 would be due to the XylID activity. XylID is known to be IlvD/EDD protein family  
361 requires an iron-sulfur cluster for its activity (Andberg et al., 2016). Functional  
362 expression of prokaryotic iron-sulfur proteins in yeast *S. cerevisiae* has been so

363 difficult because of oxygen sensibility of iron-sulfur proteins (Kirby et al. 2016), or  
364 conceivably low availability of iron-sulfur cluster (Bamba et al. 2019). Lower  
365 agitation speeds might reduce the loss of function of XylD, leading to less  
366 xylonate accumulation and increased the production of 3,4-DHBA even with  
367 lower xylose consumption.

368 Importantly, 3-HBL was also produced from xylose by spontaneous  
369 cyclization at 0.64 (200 rpm), 0.49 (300 rpm), 0.40 (400 rpm), and 0.39 g/L (500  
370 rpm) under each agitation speed, respectively (Fig. 4D). This is the first report of  
371 3-HBL production from xylose in *S. cerevisiae*, to the best of our knowledge. The  
372 previous study showed the dual production of 3,4-DHBA and 3-HBL from glucose  
373 (Dhamankar et al., 2014), but did not confirm the production of 3-HBL from xylose  
374 (Gao et al., 2017; Liu et al., 2021; Wang et al., 2017).

### 375 **3.6 | Xylonate re-assimilation led to enhanced 3,4-dihydroxybutyrate** 376 **production by engineered yeast**

377 The beneficial effects of the pH and agitation control on 3,4-DHBA production  
378 were confirmed. While xylonate accumulation reduced with the control of pH and  
379 aeration, 4.8 g/L of xylonate was still accumulated with the molar yield of 38.7 %  
380 of the consumed xylose. Previously, *C. crescentus* XylD activity was determined  
381 to be highly active under a weak alkaline condition at pH = 8.5 (Andberg et al.,  
382 2016). The optimal pH for XylD was narrow so that XylD activities drastically  
383 dropped when pH was lower than 8.5. However, in previous studies, engineered  
384 yeast strains harboring a xylose oxidative pathway with *C. crescentus* XylD have  
385 been empirically cultivated at pH  $\leq$  6.0 (Bamba et al., 2019; Borgström et al.,  
386 2019; Salusjärvi et al., 2017). As the intracellular pH of *S. cerevisiae* responds to  
387 the extracellular pH changes (Orij et al., 2009), traditional yeast fermentation at  
388 pH  $\leq$  6.0 might make XylD inactive in *S. cerevisiae*. A weak alkaline environment  
389 would enhance the heterologous XylD activity by elevating intracellular pH in *S.*



390 *cerevisiae*. However, the impacts of alkaline fermentation on xylose oxidative  
391 metabolism in *S. cerevisiae* have never been investigated so far.

392 To resolve the pH mismatch between optimal yeast growth and XylD  
393 activity, fermentations were performed while keeping a lower limit of pH in the  
394 medium at  $\text{pH} \geq 7.0$  or  $\text{pH} \geq 8.0$  by NaOH or KOH. To control the pH in the  
395 fermentation medium, NaOH or KOH was used. Glucose was consumed within  
396 24 h under all fermentation conditions (Fig. 5A). On the other hand, xylose  
397 consumption rates reduced when the pH was maintained at  $\text{pH} \geq 8.0$  as  
398 compared to when the pH was maintained at  $\text{pH} \geq 7.0$  (Fig. 5B). Interestingly,  
399 xylonate was re-assimilated from the medium into the cells under alkaline  
400 conditions and completely re-assimilated after 120 h cultivation. (Fig. 5C). This is  
401 the first observation of xylonate re-assimilation when using *S. cerevisiae* as a  
402 host strain. In all fermentations conducted under alkaline conditions, the titers of  
403 3,4-DHBA increased up to 6.5 g/L with a molar yield of 74.5 % from 10.9 g/L of  
404 xylose when pH was controlled at  $\text{pH} \geq 8.0$  using KOH (Fig. 5D). These results  
405 indicated that the weak alkaline conditions might lead to the *in vivo* activation of  
406 *C. crescentus* XylD, the re-assimilations of xylonate, and the increased  
407 productions of 3,4-DHBA production. For the efficient construction of  
408 heterologous pathway, researchers need to reconsider how heterologous  
409 enzymes are expressed in active form inside the microbial cells by the matching  
410 the optimal pH between host strain and target enzymes since the active pH range  
411 of heterologous enzymes often differs from the optimal pH of microbial host  
412 strains (Ahn et al., 2020). Unfortunately, 3-HBL production was decreased to 0.30  
413 (NaOH,  $\text{pH} \geq 7.0$ ), 0.21 (NaOH,  $\text{pH} \geq 8.0$ ), 0.37 (KOH,  $\text{pH} \geq 7.0$ ), and 0.20 g/L  
414 (KOH,  $\text{pH} \geq 8.0$ ) under alkaline conditions (Fig. S7). as compared to 0.49 g/L of  
415 3-HBL in the fermentation conducted at  $\text{pH} \geq 6.0$  using NaOH (Fig. 4D).

416 To elucidate the detailed metabolome in the 3,4-DHBA synthetic pathway,  
417 the intracellular amounts of xylonate, KDX and DHB, and extracellular amounts  
418 of KDX were measured. The intracellular amount of xylonate did not change  
419 under each fermentation conditions except for the intracellular xylonate at pH  $\geq$   
420 8.0 using KOH (Fig. 6A). In contrast, the intracellular levels of KDX and DHB were  
421 increased remarkably when the cells were cultured at pH  $\geq$  8.0 (Fig. 6B and 6C),  
422 which could be due to increased XylID activity dependent on the higher  
423 intracellular pH values. Indeed, lifting the pH in the medium from pH 6.0 to 8.0  
424 led to the increase in intracellular pH values, and XylID activity was dependent on  
425 pH from 6.0 to 8.0 (Fig. S6). Consistent with the increased level of intracellular  
426 KDX, the extracellular amount of KDX was also increased when the cells were  
427 cultured at pH  $\geq$  7.0 or at pH  $\geq$  8.0 (Fig. 6D). This indicated that putative  
428 bottlenecks in the 3,4-DHBA biosynthetic pathway might be the reaction from  
429 KDX to DHB. The expression levels of the genes involved in the 3,4-DHBA  
430 synthetic pathway did not change by changing the pH to alkaline conditions  
431 except for *xylD* (Fig. S8). Hence, this would be caused by the mismatch of the  
432 optimal pH between enzymes. For example, the optimal pH of *L. lactis* KdcA is  
433 pH 6.0 (Yep et al., 2006), which is quite different from those of *C. crescentus* XylB  
434 (pH 9.0) (Toivari et al., 2012), *C. crescentus* XylID (pH 8.5) (Andberg et al., 2016).  
435 Although the pH dependency of *E. coli* Ynel has not been reported, the enzyme  
436 is assayed at pH = 7.8 (Fuhrer et al., 2007). Thus, a weak alkaline environment  
437 would not be beneficial for all the reactions in the biosynthetic pathway.

438 When KOH was used as an alkaline reagent, xylonate accumulation was  
439 lower as compared to when NaOH was used (Fig. 5C). However, it did not have  
440 an impact on the 3,4-DHBA production. This might be caused by the low flux in  
441 the 3,4-DHBA biosynthetic pathway, leading to the accumulation of intermediates  
442 of KDX and DHB. After 72 h cultivation, intracellular levels of KDX and DHB when

443 KOH was used was 2.1- and 1.5-fold higher than those in the fermentation using  
444 NaOH at pH  $\geq$  7.0 (Fig. 6A and 6B). Moreover, KDX when using KOH was  
445 accumulated in the medium with 1.5-fold higher as compared to using NaOH (Fig.  
446 6C). Thus, the flux in the 3,4-DHBA biosynthetic pathway needs to be improved  
447 for further study.

448 In addition to the effects of pH, transporters involved in facilitating the  
449 import or export across the yeast cell membranes need to be identified for further  
450 engineering. For example, *S. cerevisiae* transports weak carboxylic acids like  
451 acetate into the cells, and the Jen family proteins, belong to the major facilitator  
452 superfamily, are identified to associate with plasma membrane transport of weak  
453 carboxylic acids in yeast (Giannattasio et al., 2013). When proteins involved in  
454 the transport of DHB, KDX and 3,4-DHBA are identified, further engineering could  
455 realize more efficient production of 3,4-DHBA with less accumulation of the  
456 intermediates.

#### 457 **4 | CONCLUSIONS**

458 This research demonstrated xylonate re-assimilation by engineered  
459 yeast for the first time. The alkaline environment is the trigger of xylonate re-  
460 assimilation, overcoming the low yields of a xylose derivative chemicals. Based  
461 on this study, we envision the implementation of a xylose oxidative pathway in  
462 yeast would be more accelerated and universally used to produce biofuels and  
463 biochemicals from lignocellulosic feedstock. Furthermore, these results provide  
464 new insights into the reduction and re-assimilation of intermediates, as well as  
465 how the heterologous pathway works in the host strain to match the active pH  
466 range of host strain and target enzyme.

467

468 **REFERENCE**

- 469 Ahn, J. H., Seo, H., Park, W., Seok, J., Lee, J. A., Kim, W. J., Kim, G. B., Kim,  
470 K.-J., & Lee, S. Y. (2020). Enhanced succinic acid production by *Mannheimia*  
471 employing optimal malate dehydrogenase. *Nature Communications*, *11*(1), 1970.  
472 <https://doi.org/10.1038/s41467-020-15839-z>
- 473 Andberg, M., Aro-Kärkkäinen, N., Carlson, P., Oja, M., Bozonnet, S., Toivari, M.,  
474 Hakulinen, N., O'Donohue, M., Penttilä, M., & Koivula, A. (2016).  
475 Characterization and mutagenesis of two novel iron–sulphur cluster pentonate  
476 dehydratases. *Applied Microbiology and Biotechnology*, *100*(17), 7549–7563.  
477 <https://doi.org/10.1007/s00253-016-7530-8>
- 478 Bai, W., Tai, Y.-S., Wang, J., Wang, J., Jambunathan, P., Fox, K. J., & Zhang, K.  
479 (2016). Engineering nonphosphorylative metabolism to synthesize mesaconate  
480 from lignocellulosic sugars in *Escherichia coli*. *Metabolic Engineering*, *38*, 285–  
481 292. <https://doi.org/10.1016/j.ymben.2016.09.007>
- 482 Bamba, T., Yukawa, T., Guirimand, G., Inokuma, K., Sasaki, K., Hasunuma, T.,  
483 & Kondo, A. (2019). Production of 1,2,4-butanetriol from xylose by  
484 *Saccharomyces cerevisiae* through Fe metabolic engineering. *Metabolic*  
485 *Engineering*, *56*, 17–27. <https://doi.org/10.1016/j.ymben.2019.08.012>
- 486 Bañares, A. B., Nisola, G. M., Valdehuesa, K. N. G., Lee, W.-K., & Chung, W.-J.  
487 (2021). Understanding D-xylonic acid accumulation: A cornerstone for better  
488 metabolic engineering approaches. *Applied Microbiology and Biotechnology*,  
489 *105*(13), 5309–5324. <https://doi.org/10.1007/s00253-021-11410-y>
- 490 Borgström, C., Wasserstrom, L., Almqvist, H., Broberg, K., Klein, B., Noack, S.,  
491 Lidén, G., & Gorwa-Grauslund, M. F. (2019). Identification of modifications  
492 procuring growth on xylose in recombinant *Saccharomyces cerevisiae* strains  
493 carrying the Weimberg pathway. *Metabolic Engineering*, *55*, 1–11.  
494 <https://doi.org/10.1016/j.ymben.2019.05.010>

495 Brüsseler, C., Späth, A., Sokolowsky, S., & Marienhagen, J. (2019). Alone at last!  
496 – Heterologous expression of a single gene is sufficient for establishing the five-  
497 step Weimberg pathway in *Corynebacterium glutamicum*. *Metabolic Engineering*  
498 *Communications*, 9, e00090. <https://doi.org/10.1016/j.mec.2019.e00090>

499 Calahorra, M., Martínez, G. A., Hernández-Cruz, A., & Peña, A. (1998). Influence  
500 of monovalent cations on yeast cytoplasmic and vacuolar pH. *Yeast*, 14(6), 501–  
501 515. [https://doi.org/10.1002/\(SICI\)1097-0061\(19980430\)14:6<501::AID-](https://doi.org/10.1002/(SICI)1097-0061(19980430)14:6<501::AID-)  
502 [YEA249>3.0.CO;2-6](https://doi.org/10.1002/(SICI)1097-0061(19980430)14:6<501::AID-YEA249>3.0.CO;2-6)

503 Choi, S. Y., Park, S. J., Kim, W. J., Yang, J. E., Lee, H., Shin, J., & Lee, S. Y.  
504 (2016). One-step fermentative production of poly(lactate-co-glycolate) from  
505 carbohydrates in *Escherichia coli*. *Nature Biotechnology*, 34(4), 435–440.  
506 <https://doi.org/10.1038/nbt.3485>

507 Dahms, A.S., (1974). 3-Deoxy-D-pentulosonic acid aldolase and its role in a new  
508 pathway of D-xylose degradation. *Biochem. Biophys. Res. Commun.* 60, 1433–  
509 1439

510 de Smidt, O., du Preez, J. C., & Albertyn, J. (2008). The alcohol dehydrogenases  
511 of *Saccharomyces cerevisiae*: A comprehensive review. *FEMS Yeast Research*,  
512 8(7), 967–978. <https://doi.org/10.1111/j.1567-1364.2008.00387.x>

513 Dhamankar, H., Tarasova, Y., Martin, C. H., & Prather, K. L. J. (2014).  
514 Engineering *E. coli* for the biosynthesis of 3-hydroxy- $\gamma$ -butyrolactone (3HBL) and  
515 3,4-dihydroxybutyric acid (3,4-DHBA) as value-added chemicals from glucose as  
516 a sole carbon source. *Metabolic Engineering*, 25, 72–81.  
517 <https://doi.org/10.1016/j.ymben.2014.06.004>

518 Fuhrer, T., Chen, L., Sauer, U., & Vitkup, D. (2007). Computational Prediction  
519 and Experimental Verification of the Gene Encoding the NAD<sup>+</sup>/NADP<sup>+</sup>-  
520 Dependent Succinate Semialdehyde Dehydrogenase in *Escherichia coli*. *Journal*  
521 *of Bacteriology*, 189(22), 8073–8078. <https://doi.org/10.1128/JB.01027-07>

522 Fujiwara, R., Noda, S., Tanaka, T., & Kondo, A. (2020). Metabolic engineering of  
523 *Escherichia coli* for shikimate pathway derivative production from glucose–xylose  
524 co-substrate. *Nature Communications*, 11(1), 279.  
525 <https://doi.org/10.1038/s41467-019-14024-1>

526 Gao, H., Gao, Y., & Dong, R. (2017). Enhanced biosynthesis of 3,4-  
527 dihydroxybutyric acid by engineered *Escherichia coli* in a dual-substrate system.  
528 *Bioresource Technology*, 245, 794–800.  
529 <https://doi.org/10.1016/j.biortech.2017.09.017>

530 Giannattasio, S., Guaragnella, N., Ždravlević, M., & Marra, E. (2013). Molecular  
531 mechanisms of *Saccharomyces cerevisiae* stress adaptation and programmed  
532 cell death in response to acetic acid. *Frontiers in Microbiology*, 4.  
533 <https://doi.org/10.3389/fmicb.2013.00033>

534 Hasunuma, T., Kikuyama, F., Matsuda, M., Aikawa, S., Izumi, Y., & Kondo, A.  
535 (2013). Dynamic metabolic profiling of cyanobacterial glycogen biosynthesis  
536 under conditions of nitrate depletion. *Journal of Experimental Botany*, 64(10),  
537 2943–2954. <https://doi.org/10.1093/jxb/ert134>

538 Hensing, M. C. M., Bangma, K. A., Raamsdonk, L. M., de Hulster, E., van Dijken,  
539 J. P., & Pronk, J. T. (1995). Effects of cultivation conditions on the production of  
540 heterologous  $\alpha$ -galactosidase by *Kluyveromyces lactis*. *Applied Microbiology and*  
541 *Biotechnology*, 43(1), 58–64. <https://doi.org/10.1007/BF00170623>

542 Hong, K.-K., & Nielsen, J. (2012). Metabolic engineering of *Saccharomyces*  
543 *cerevisiae*: A key cell factory platform for future biorefineries. *Cellular and*  
544 *Molecular Life Sciences*, 69(16), 2671–2690. [https://doi.org/10.1007/s00018-](https://doi.org/10.1007/s00018-012-0945-1)  
545 [012-0945-1](https://doi.org/10.1007/s00018-012-0945-1)

546 Inokuma, K., Matsuda, M., Sasaki, D., Hasunuma, T., & Kondo, A. (2018).  
547 Widespread effect of N-acetyl-d-glucosamine assimilation on the metabolisms of

548 amino acids, purines, and pyrimidines in *Scheffersomyces stipitis*. *Microbial Cell*  
549 *Factories*, 17. <https://doi.org/10.1186/s12934-018-0998-4>

550 Kim, S. R., Park, Y.-C., Jin, Y.-S., & Seo, J.-H. (2013). Strain engineering of  
551 *Saccharomyces cerevisiae* for enhanced xylose metabolism. *Biotechnology*  
552 *Advances*, 31(6), 851–861. <https://doi.org/10.1016/j.biotechadv.2013.03.004>

553 Kirby, J., Dietzel, K. L., Wichmann, G., Chan, R., Antipov, E., Moss, N., Baidoo,  
554 E. E. K., Jackson, P., Gaucher, S. P., Gottlieb, S., LaBarge, J., Mahatdejkul, T.,  
555 Hawkins, K. M., Muley, S., Newman, J. D., Liu, P., Keasling, J. D., & Zhao, L.  
556 (2016). Engineering a functional 1-deoxy-D-xylulose 5-phosphate (DXP) pathway  
557 in *Saccharomyces cerevisiae*. *Metabolic Engineering*, 38, 494–503.  
558 <https://doi.org/10.1016/j.ymben.2016.10.017>

559 Kumánovics, A., Chen, O. S., Li, L., Bagley, D., Adkins, E. M., Lin, H., Dingra, N.  
560 N., Outten, C. E., Keller, G., Winge, D., Ward, D. M., & Kaplan, J. (2008).  
561 Identification of *FRA1* and *FRA2* as Genes Involved in Regulating the Yeast Iron  
562 Regulon in Response to Decreased Mitochondrial Iron-Sulfur Cluster Synthesis.  
563 *Journal of Biological Chemistry*, 283(16), 10276–10286.  
564 <https://doi.org/10.1074/jbc.M801160200>

565 Lane, S., Dong, J., & Jin, Y.-S. (2018). Value-added biotransformation of  
566 cellulosic sugars by engineered *Saccharomyces cerevisiae*. *Bioresource*  
567 *Technology*, 260, 380–394. <https://doi.org/10.1016/j.biortech.2018.04.013>

568 Larroy, C., Fernández, M. R., González, E., Parés, X., & Biosca, J. A. (2002).  
569 Characterization of the *Saccharomyces cerevisiae* YMR318C (*ADH6*) gene  
570 product as a broad specificity NADPH-dependent alcohol dehydrogenase:  
571 Relevance in aldehyde reduction. *Biochemical Journal*, 361(Pt 1), 163–172.

572 Larroy, C., Parés, X., & Biosca, J. A. (2002). Characterization of a  
573 *Saccharomyces cerevisiae* NADP(H)-dependent alcohol dehydrogenase  
574 (ADHVII), a member of the cinnamyl alcohol dehydrogenase family. *European*

575 *Journal of Biochemistry*, 269(22), 5738–5745. <https://doi.org/10.1046/j.1432->  
576 1033.2002.03296.x

577 Lee, Y., Kim, C., Sun, L., Lee, T., & Jin, Y. (2022). Selective production of retinol  
578 by engineered *Saccharomyces cerevisiae* through the expression of retinol  
579 dehydrogenase. *Biotechnology and Bioengineering*, 119(2), 399–410.  
580 <https://doi.org/10.1002/bit.28004>

581 Li, L., Jia, X., Ward, D. M., & Kaplan, J. (2011). Yap5 Protein-regulated  
582 Transcription of the *TYW1* Gene Protects Yeast from High Iron Toxicity. The  
583 *Journal of Biological Chemistry*, 286(44), 38488–38497.  
584 <https://doi.org/10.1074/jbc.M111.286666>

585 Liu, Y., Mao, X., Zhang, B., Lin, J., & Wei, D. (2021). Modification of an  
586 engineered *Escherichia coli* by a combinatorial strategy to improve 3,4-  
587 dihydroxybutyric acid production. *Biotechnology Letters*, 43(10), 2035–2043.  
588 <https://doi.org/10.1007/s10529-021-03169-z>

589 Martin, C. H., Dhamankar, H., Tseng, H.-C., Sheppard, M. J., Reisch, C. R., &  
590 Prather, K. L. J. (2013). A platform pathway for production of 3-hydroxyacids  
591 provides a biosynthetic route to 3-hydroxy- $\gamma$ -butyrolactone. *Nature*  
592 *Communications*, 4(1). <https://doi.org/10.1038/ncomms2418>

593 Niu, W., Molefe, M. N., & Frost, J. W. (2003). Microbial Synthesis of the Energetic  
594 Material Precursor 1,2,4-Butanetriol. 2.

595 Orij, R., Postmus, J., Ter Beek, A., Brul, S., & Smits, G. J. (2009). *In vivo*  
596 measurement of cytosolic and mitochondrial pH using a pH-sensitive GFP  
597 derivative in *Saccharomyces cerevisiae* reveals a relation between intracellular  
598 pH and growth. *Microbiology*, 155(1), 268–278.  
599 <https://doi.org/10.1099/mic.0.022038-0>

600 Peña, A., Sánchez, N. S., Álvarez, H., Calahorra, M., & Ramírez, J. (2015).  
601 Effects of high medium pH on growth, metabolism and transport in



602 *Saccharomyces cerevisiae*. *FEMS Yeast Research*, 15(2).  
603 <https://doi.org/10.1093/femsyr/fou005>

604 Protzko, R. J., Latimer, L. N., Martinho, Z., de Reus, E., Seibert, T., Benz, J. P.,  
605 & Dueber, J. E. (2018). Engineering *Saccharomyces cerevisiae* for co-utilization  
606 of d-galacturonic acid and d-glucose from citrus peel waste. *Nature*  
607 *Communications*, 9(1). <https://doi.org/10.1038/s41467-018-07589-w>

608 Reifenrath, M., & Boles, E. (2018). A superfolder variant of pH-sensitive pHluorin  
609 for *in vivo* pH measurements in the endoplasmic reticulum. *Scientific Reports*,  
610 8(1), 11985. <https://doi.org/10.1038/s41598-018-30367-z>

611 Salusjärvi, L., Toivari, M., Vehkomäki, M.-L., Koivistoinen, O., Mojzita, D.,  
612 Niemelä, K., Penttilä, M., & Ruohonen, L. (2017). Production of ethylene glycol  
613 or glycolic acid from D-xylose in *Saccharomyces cerevisiae*. *Applied Microbiology*  
614 *and Biotechnology*, 101(22), 8151–8163. [https://doi.org/10.1007/s00253-017-](https://doi.org/10.1007/s00253-017-8547-3)  
615 8547-3

616 Sharma, J., Kumar, V., Prasad, R., & Gaur, N. A. (2022). Engineering of  
617 *Saccharomyces cerevisiae* as a consolidated bioprocessing host to produce  
618 cellulosic ethanol: Recent advancements and current challenges. *Biotechnology*  
619 *Advances*, 56, 107925. <https://doi.org/10.1016/j.biotechadv.2022.107925>

620 Shen, L., Kohlhaas, M., Enoki, J., Meier, R., Schönenberger, B., Wohlgemuth, R.,  
621 Kourist, R., Niemeyer, F., van Niekerk, D., Bräsen, C., Niemeyer, J., Snoep, J.,  
622 & Siebers, B. (2020). A combined experimental and modelling approach for the  
623 Weimberg pathway optimization. *Nature Communications*, 11(1), 1098.  
624 <https://doi.org/10.1038/s41467-020-14830-y>

625 Sun, L., Lee, J. W., Yook, S., Lane, S., Sun, Z., Kim, S. R., & Jin, Y.-S. (2021).  
626 Complete and efficient conversion of plant cell wall hemicellulose into high-value  
627 bioproducts by engineered yeast. *Nature Communications*, 12(1), 4975.  
628 <https://doi.org/10.1038/s41467-021-25241-y>

629 Tai, Y.-S., Xiong, M., Jambunathan, P., Wang, J., Wang, J., Stapleton, C., &  
630 Zhang, K. (2016). Engineering nonphosphorylative metabolism to generate  
631 lignocellulose-derived products. *Nature Chemical Biology*, *12*(4), 247–253.  
632 <https://doi.org/10.1038/nchembio.2020>

633 Toivari, M. H., Nygård, Y., Penttilä, M., Ruohonen, L., & Wiebe, M. G. (2012).  
634 Microbial d-xylonate production. *Applied Microbiology and Biotechnology*, *96*(1),  
635 1–8. <https://doi.org/10.1007/s00253-012-4288-5>

636 Toivari, M., Nygård, Y., Kumpula, E.-P., Vehkomäki, M.-L., Benčina, M.,  
637 Valkonen, M., Maaheimo, H., Andberg, M., Koivula, A., Ruohonen, L., Penttilä,  
638 M., & Wiebe, M. G. (2012). Metabolic engineering of *Saccharomyces cerevisiae*  
639 for bioconversion of d-xylose to d-xylonate. *Metabolic Engineering*, *14*(4), 427–  
640 436. <https://doi.org/10.1016/j.ymben.2012.03.002>

641 Wang, J., Shen, X., Jain, R., Wang, J., Yuan, Q., & Yan, Y. (2017). Establishing  
642 a novel biosynthetic pathway for the production of 3,4-dihydroxybutyric acid from  
643 xylose in *Escherichia coli*. *Metabolic Engineering*, *41*, 39–45.  
644 <https://doi.org/10.1016/j.ymben.2017.03.003>

645 Watanabe, S., Fukumori, F., Nishiwaki, H., Sakurai, Y., Tajima, K., & Watanabe,  
646 Y. (2019). Novel non-phosphorylative pathway of pentose metabolism from  
647 bacteria. *Scientific Reports*, *9*(1), 155. [https://doi.org/10.1038/s41598-018-](https://doi.org/10.1038/s41598-018-36774-6)  
648 [36774-6](https://doi.org/10.1038/s41598-018-36774-6)

649 Wei, N., Quarterman, J., Kim, S. R., Cate, J. H. D., & Jin, Y.-S. (2013). Enhanced  
650 biofuel production through coupled acetic acid and xylose consumption by  
651 engineered yeast. *Nature Communications*, *4*(1), 2580.  
652 <https://doi.org/10.1038/ncomms3580>

653 Weimberg, R., (1961). Pentose oxidation by *Pseudomonas fragi*. *J. Biol. Chem.*  
654 *236*, 629–635.

655 Werpy, T., & Petersen, G. (2004). Top Value Added Chemicals from Biomass:  
656 Volume I -- Results of Screening for Potential Candidates from Sugars and  
657 Synthesis Gas (DOE/GO-102004-1992, 15008859).  
658 <https://doi.org/10.2172/15008859>

659 Yep, A., Kenyon, G. L., & McLeish, M. J. (2006). Determinants of substrate  
660 specificity in KdcA, a thiamin diphosphate-dependent decarboxylase. *Bioorganic*  
661 *Chemistry*, 34(6), 325–336. <https://doi.org/10.1016/j.bioorg.2006.08.005>

662 Yukawa, T., Bamba, T., Guirimand, G., Matsuda, M., Hasunuma, T., & Kondo, A.  
663 (2021). Optimization of 1,2,4 - butanetriol production from xylose in  
664 *Saccharomyces cerevisiae* by metabolic engineering of NADH/NADPH balance.  
665 *Biotechnology and Bioengineering*, 118(1), 175–185.  
666 <https://doi.org/10.1002/bit.27560>

667

668

669 **Table captions:**

670 **Table 1** Strain used in the present study.

671

672 **Table 2** The biochemical production by microorganisms via a xylose oxidative  
673 pathway

674

675 **Figure captions:**

676 **Fig. 1**

677 Overview of the xylose oxidative pathway. KDX, 2-Keto-3-deoxy-xylonate;  
678 AKGSA,  $\alpha$ -Ketoglutarate semialdehyde; AKG,  $\alpha$ -Ketoglutarate; EG, Ethylene  
679 glycol; DHB, 3,4-Dihydroxybutanal; 3,4-DHBA, 3,4-Dihydroxybutyrate; 3-HBL, 3-  
680 Hydroxybutylolactone; XylB, Xylose dehydrogenase; XylD, Xylonate  
681 dehydratase; XylX, 2-Keto-3-deoxy-xylonate dehydratase; XylA,  $\alpha$ -Ketoglutarate  
682 semialdehyde dehydrogenase; YjhH and YagG, KDX aldolase, ALD, aldehyde  
683 dehydrogenase; ADH, alcohol dehydrogenase; Kdc, 2-ketoacid decarboxylase.

684

685 **Fig. 2**

686 The effects of ADH gene disruption on (A) xylose consumption and (B) BT  
687 production by the BDK (orange, dot circle), BDK $\Delta$ 1 (red, squares), BDK $\Delta$ 2 (blue,  
688 rhombuses), BDK $\Delta$ 3 (green, triangles), BDK $\Delta$ 4 (purple, crosses), BDK $\Delta$ 5 (light  
689 yellow, bars) BDK $\Delta$ 6 (black, circles), BDK $\Delta$ 7 (brown, asterisks) with disruption of  
690 each ADH gene. (C) The time-course profiles of BT production and (D) 3,4-DHBA  
691 production during the glucose and xylose co-fermentation by the BD $\delta$ K603  
692 (control, green triangles) and BD $\delta$ K604 (*ADH6* deletion, red squares) strains. The  
693 fermentation medium contained 10 g/L glucose and 10 g/L xylose. Error bars  
694 indicate standard deviations from three independent experiments.

695

696 **Fig. 3**

697 The time-course profiles of (A) 3,4-DHBA production and (B) xylonate  
698 accumulation by engineered *S. cerevisiae* strains expressing different ALDs.  
699 BD $\delta$ K604-Ynel (blue, circles), BD $\delta$ K604-Uga2 (orange, crosses), BD $\delta$ K604-Ald2  
700 (purple, triangles), and BD $\delta$ K604-Ald3 (light yellow, asterisks). The shake-flask  
701 fermentations were performed in the YP medium containing 10 g/L glucose and  
702 10 g/L of xylose. (C) Time-course of pH change during the fermentation of  
703 BD $\delta$ K604-Ynel (green). The optimal pH range of *S. cerevisiae* for growth is  
704 shown in grey range. Error bars indicate standard deviations from three  
705 independent experiments.

706

707 **Fig. 4**

708 The effects of different agitation rates on (A) xylose consumption, (B) xylonate  
709 accumulation, and (C) 3,4-DHBA production by the BD $\delta$ K604-Ynel strain under  
710 the pH control using a bioreactor. Agitation speeds were changed at 200 rpm  
711 (orange, squares), 300 rpm (red, circles), 400 rpm (blue, rhombuses), and 500  
712 rpm (green, triangles) at pH  $\geq$  6.0. (D) The 3-HBL productions by the BD $\delta$ K604-  
713 Ynel strain under the different agitation speeds (200 rpm, 300 rpm, 400 rpm, and  
714 500 rpm) at pH  $\geq$  6.0. The engineered yeast was cultivated in the YP medium  
715 containing 10 g/L of glucose and 10 g/L of xylose, and the pH of fermentation  
716 medium was maintained at pH  $\geq$  6.0 using 5 N NaOH. Error bars indicate  
717 standard deviations from two independent experiments.

718

719 **Fig. 5**

720 Time-course profiles of (A) glucose consumption, (B) xylose consumption, (C)  
721 xylonate accumulation, and (D) 3,4-DHBA production by the BD $\delta$ K604-Ynel  
722 strain during the pH-controlled fermentation using a bioreactor. The

723 fermentations were performed under the alkaline conditions at  $\text{pH} \geq 7.0$  using  
724 NaOH (orange, squares) and 8.0 using NaOH (red, rhombuses), or at  $\text{pH} \geq 7.0$   
725 using KOH (blue, triangles), and 8.0 using KOH (green, circles) in the YP medium  
726 containing 10 g/L of glucose and 10 g/L of xylose. Error bars indicate standard  
727 deviations from two independent experiments.

728

729 **Fig. 6**

730 The amounts of (A) intracellular xylonate and (B) the relative amounts of  
731 intracellular KDX, (C) intracellular DHB, and (D) extracellular KDX when re-  
732 assimilating xylonate from the medium into the cells of the BD $\delta$ K604-Ynel strain.  
733 The fermentations were performed at  $\text{pH} \geq 7.0$  or 8.0 using NaOH or KOH in the  
734 YP medium containing 10 g/L of glucose and 10 g/L of xylose. Blue and orange  
735 bar indicates the sample at 72 h and 96 h, respectively. The relative amounts  
736 were shown as a fold change in the metabolites amount at 72 h at  $\text{pH} \geq 6.0$  by  
737 NaOH. Error bars indicate standard deviations from two independent  
738 experiments.

739

Strain Name	Description	Reference
YPH499	<i>MATa ura3 - 52 lys2 - 801 ade2 - 101 trp1 - 63 his3 - Δ200 le</i>	Stratagene
YPH499 ΔGRE3	YPH499, <i>gre3Δ::kanMX</i>	Bamba et al. 2019
BDK	YPH499, pTs-A-xyIBD-kdcA	This study
BDKΔ1	BDK, <i>ADH1Δ::KanMX</i>	This study
BDKΔ2	BDK, <i>ADH2Δ::KanMX</i>	This study
BDKΔ3	BDK, <i>ADH3Δ::KanMX</i>	This study
BDKΔ4	BDK, <i>ADH4Δ::KanMX</i>	This study
BDKΔ5	BDK, <i>ADH5Δ::KanMX</i>	This study
BDKΔ6	BDK, <i>ADH6Δ::KanMX</i>	This study
BDKΔ7	BDK, <i>ADH7Δ::KanMX</i>	This study
BDδK603	YPH499 ΔGRE3, <i>tdh3p-CcxyIB</i> , <i>sed1p-CcxyID</i> , six copies of <i>L. lactis kdcA</i> , <i>bol2Δ::HIS3</i> , <i>pgk1p-tTYW1</i>	Yukawa et al. 2021
BDδK604	BDδK603, <i>ADH6Δ::1 kbp fragment</i>	This study
BDδK604-Ynel	BDδK604, <i>pIL-tdh3p-Ec_ynel-adh1t</i>	This study
BDδK604-Uga2	BDδK604, <i>pIL-tdh3p-Sc_UGA2-adh1t</i>	This study
BDδK604-Ald2	BDδK604, <i>pIL-tdh3p-Sc_ALD2-adh1t</i>	This study
BDδK604-Ald3	BDδK604, <i>pIL-tdh3p-Sc_ALD3-adh1t</i>	This study
Ynel-sfpHluorin	BDδK604-Ynel, <i>pIU-pTDH3-sfpHluorin-tADH1</i>	This study
Uga2-sfpHluorin	BDδK604-Uga2, <i>pIU-pTDH3-sfpHluorin-tADH1</i>	This study
Ald2-sfpHluorin	BDδK604-Ald2, <i>pIL-pTDH3-sfpHluorin-tADH1</i>	This study
Ald3-sfpHluorin	BDδK604-Ald3, <i>pIL-pTDH3-sfpHluorin-tADH1</i>	This study

<b>Host</b>	<b>Carbon source</b>	<b>Target Products</b>	<b>Mode of culuture</b>	<b>Titer</b>	<b>Yield</b>	<b>Reference</b>
<i>Escherichia coli</i>	20 g/L Xylose	3,4-DHBA	Batch, Flask	1.27 g/L	Not determined	Wang et al. 2017
<i>Escherichia coli</i>	5 g/L Glucose and 20 g/L Xylose	3,4-DHBA	Batch, Flask	0.38 g/L	Not determined	Gao et al. 2017
<i>Escherichia coli</i>	20 g/L Xylose	3,4-DHBA	Batch, Flask	7.71 g/L	60%	Liu et al. 2021
<i>Saccharomyces cerevisiae</i>	10 g/L glucose and 20 g/L Xylose	Glycolate	Batch, Flask	1.0 g/L	Not determined	Salusjärvi et al. 2017
<i>Saccharomyces cerevisiae</i>	10 g/L glucose and 10 g/L xylose	1,2,4-butanetriol	Batch, Flask	1,7 g/L	25%	Bamba et al. 2019
<i>Saccharomyces cerevisiae</i>	10 g/L glucose and 10 g/L xylose feeding glucose and xylose	1,2,4-butanetriol	Fed-batch, Bioreactor (pH ≥ 5.5)	6.6 g/L	57%	Yukawa et al. 2021
<i>Saccharomyces cerevisiae</i>	10 g/L glucose and 10 g/L xylose	3,4-DHBA, 3-HBL	Batch, Bioreactor (pH≥ 8.0)	6.5 g/L (3,4-DHBA) 0.2 g/L (3-HBL)	79%	This study



Fig. 1

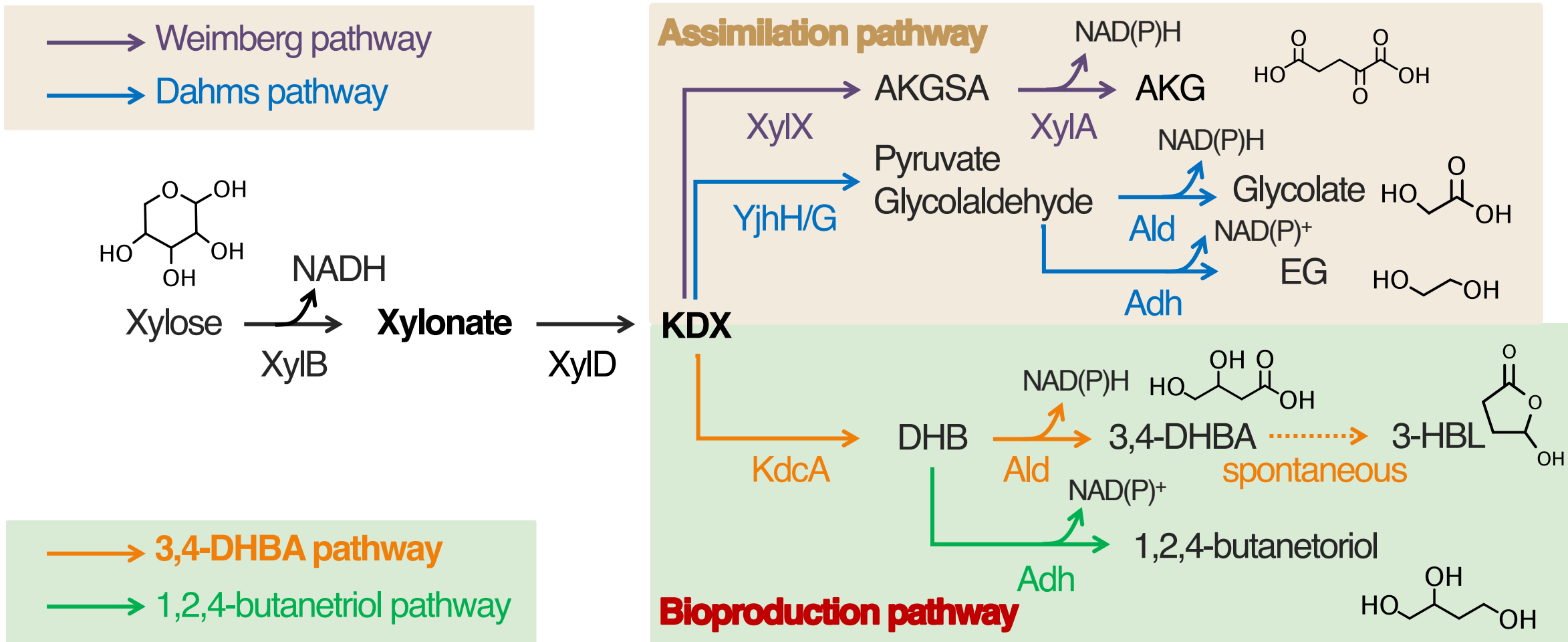


Figure 2

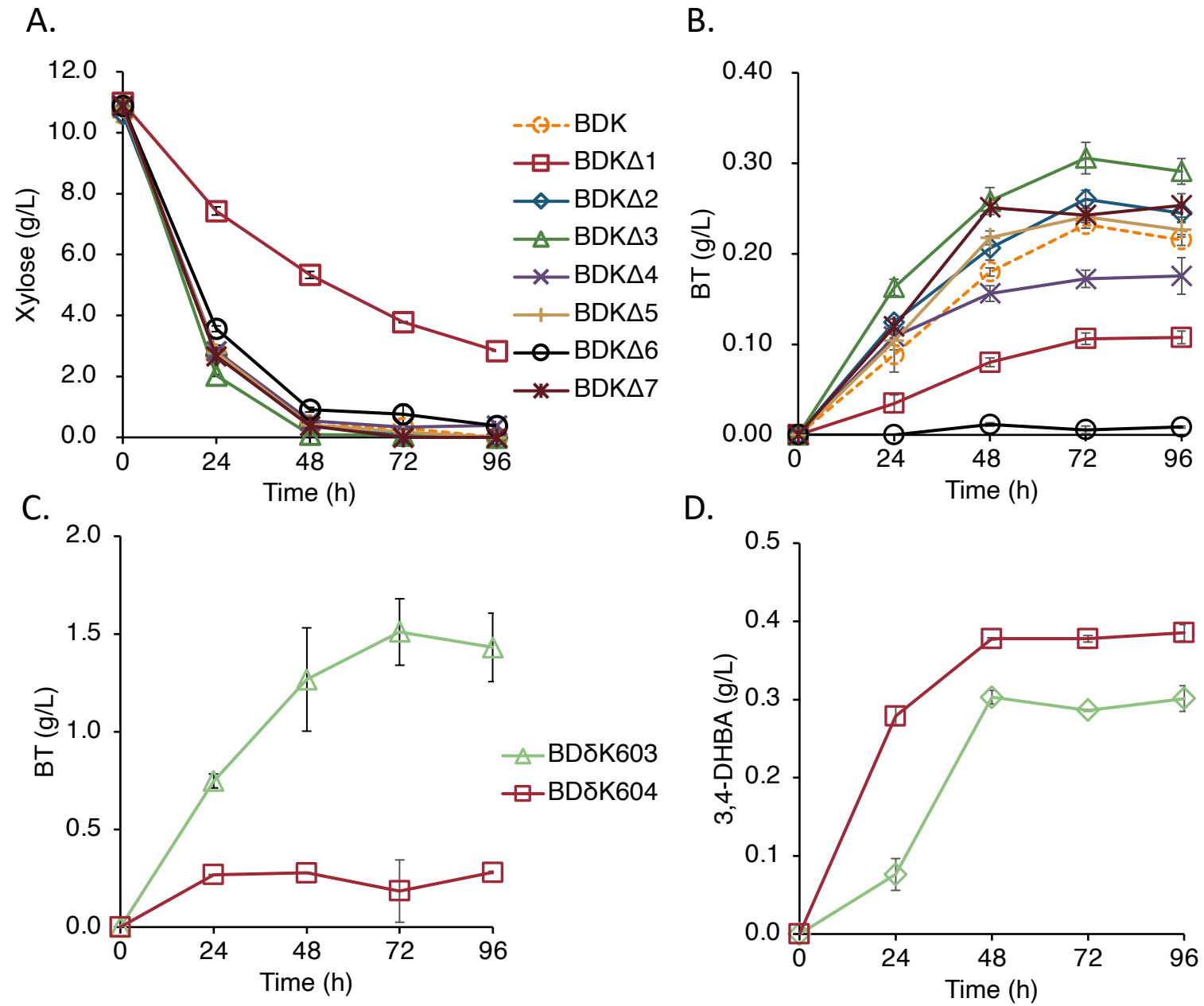


Figure 3

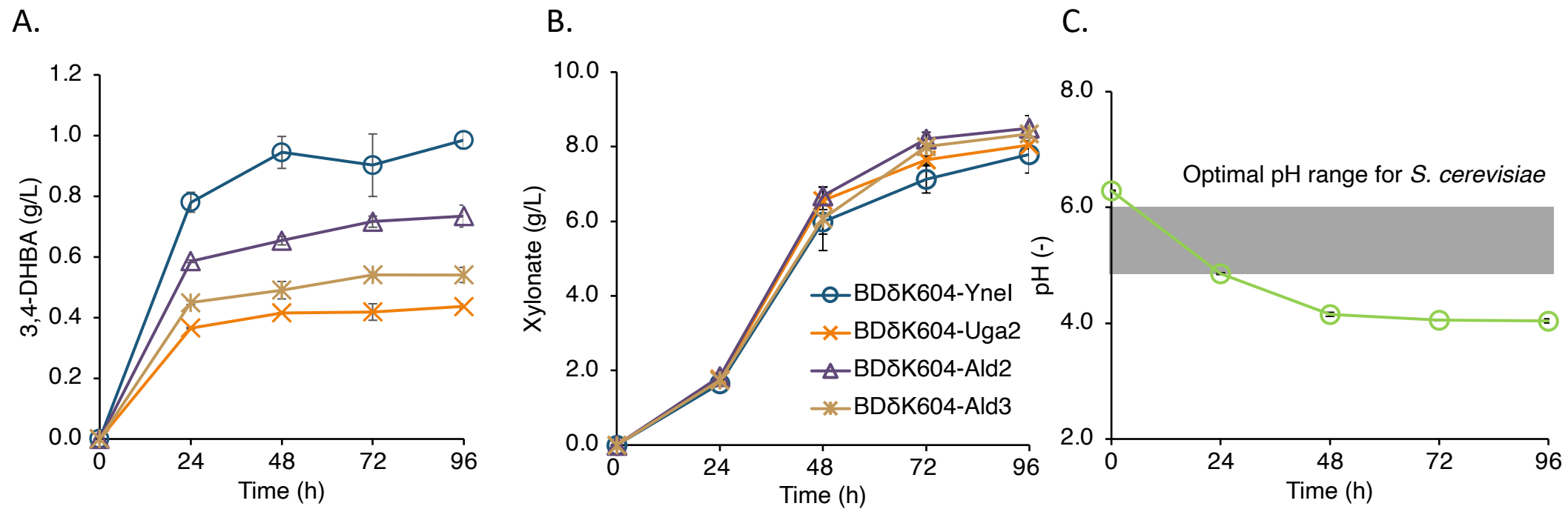


Figure 4

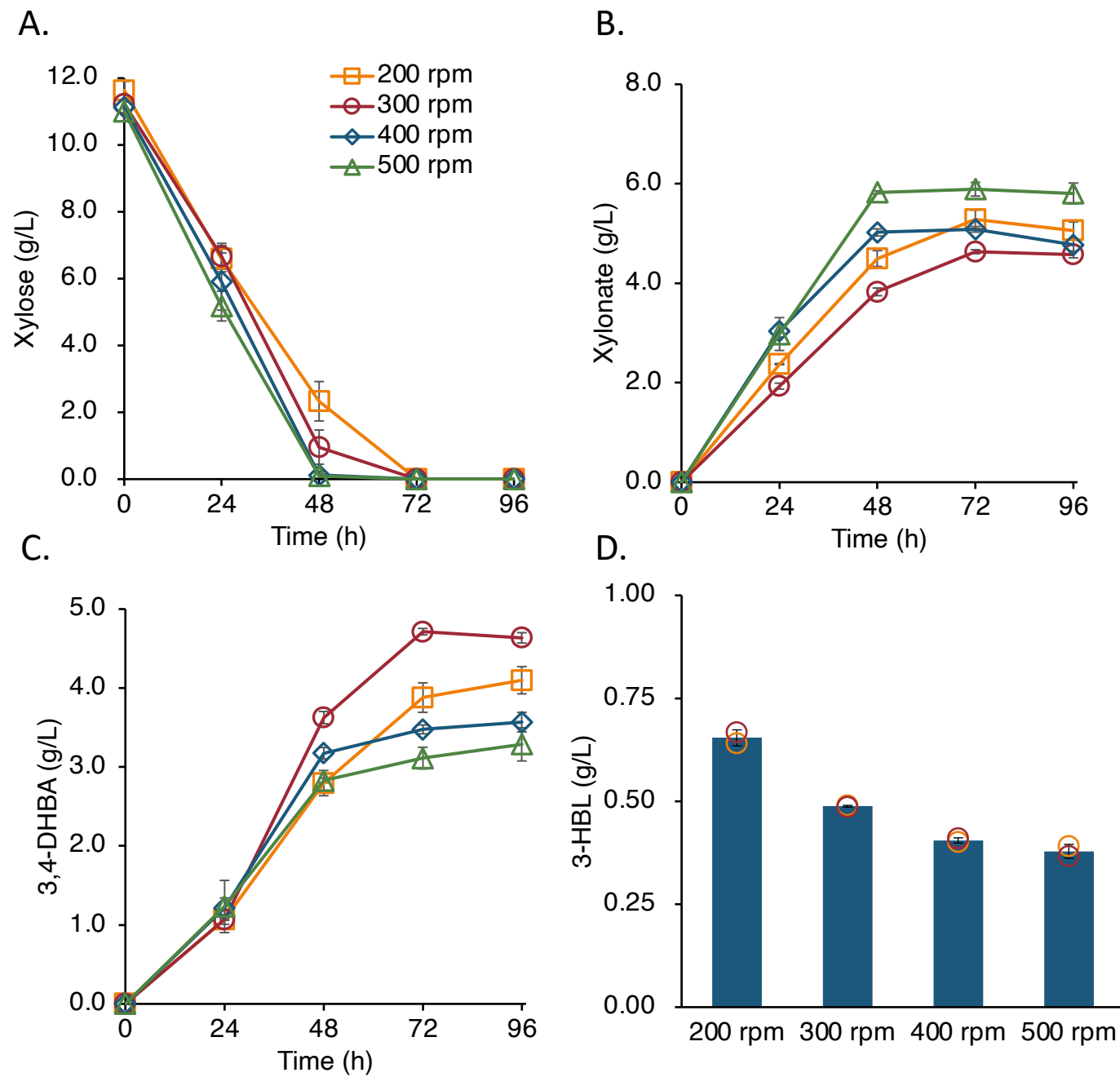


Figure 5

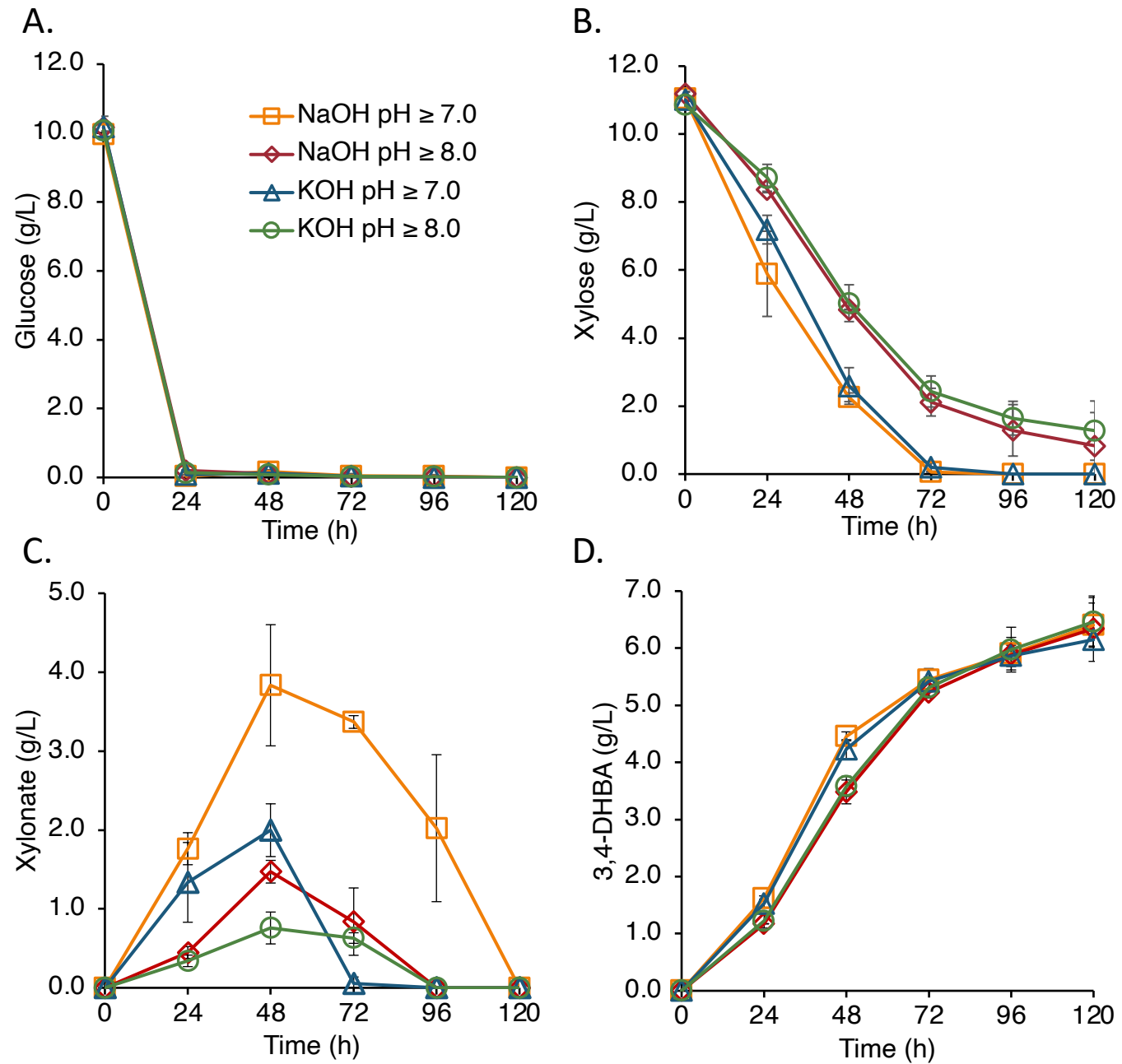


Figure 6

